Structural and Electronic Properties of Au and Au2 on an MgO(100) Surface: A DFT Cluster Embedding Approach

ARTICLE *in* THE JOURNAL OF PHYSICAL CHEMISTRY C · AUGUST 2008

Impact Factor: 4.77 · DOI: 10.1021/jp804355z

5 AUTHORS, INCLUDING:

Carlos Quintanar
Universidad Nacional Autónoma de México
23 PUBLICATIONS **139** CITATIONS
SEE PROFILE

Jose Ulises Reveles
Virginia Commonwealth University
76 PUBLICATIONS **1,388** CITATIONS
SEE PROFILE

Structural and Electronic Properties of Au and Au_2 on an MgO(100) Surface: A DFT Cluster Embedding Approach

Reyna Caballero,[†,‡] Carlos Quintanar,[†,*] Andreas M. Köster,[§] Shiv N. Khanna,[||] and J. Ulises Reveles*[,||]

Facultad de Ciencias, Universidad Nacional Autónoma de México, Ciudad Universitaria, 04510 México, D.F., México, Departamento de Supercómputo, DGSCA, Universidad Nacional Autónoma de México, Ciudad Universitaria, 04510, México, D.F., México, Departamento de Química, Cinvestav, Avenida Instituto Politécnico Nacional 2508, A.P. 14-740, México, D.F., 07000, México, and Physics Department, Virginia Commonwealth University, Richmond, Virginia, 23284-2000

Received: May 16, 2008

The structural and electronic properties of Au and Au_2 adsorbed on five coordinated oxygen and magnesium regular terrace sites, on the neutral F_s color center (oxygen vacancy containing two electrons), and on the charged F_s^+ color center (oxygen vacancy containing one electron) of the MgO(100) surface have been investigated using a density functional theory cluster embedding approach. Two types of calculations have been performed. In one, we optimized and calculated the energetics of the systems using a generalized gradient approximation, and in the second, we used a combined approach, optimizing the geometries using a local density approximation and then performing a single point energy calculation using a generalized gradient approximation. Our studies also examine the effect of relaxation of the substrate. This was accomplished through two studies: first, both the MgO surface and the Au atoms were optimized, and second, the MgO surface atoms were kept fixed while the Au atoms were allowed to relax. We report the geometry, adsorption, and dimerization energies of the lowest energy and low energy isomers at each adsorption site, charge transfers from the MgO surface to the Au atoms in the lowest energy isomers, and compare our findings with previous theoretical studies. This comparison allowed us to establish in most of the cases limits for the adsorption energies, binding energies, and geometrical parameters at each adsorption site. For the case of Au_2, for each adsorption site, our studies confirm the lowest energy isomer and most of the low energy isomers, previously reported, when both the surface and the Au_2 are optimized. For most cases, the studies with frozen MgO surface atoms produced similar results as the studies when the MgO surface atoms were optimized. However, for the Mg site we found that the restrictions introduced by keeping the surface frozen favored the coexistence of an additional low energy isomer, and for the F_s^+ site, the restrictions favored the dissociation of the adsorbed Au_2 dimer into two surface adsorbed Au atoms. In general, both fully generalized gradient and combined calculations produced similar results, though, in the case of the F_s site the combined calculations found another low lying isomer, and in the case of the F_s^+ site it predicted the dissociation of the adsorbed Au_2 dimer, and inverted the energetic order of the lowest energy and low energy isomers. An increase in the charge transfer from the MgO surface to the Au atoms at the different adsorption sites according with the number of localized electrons at the adsorption sites was found. Finally, we found that the site with the largest adsorption and dimerization energies, and where an Au atom is most stable and can grow, is the neutral F_s center.

I. Introduction

Nanoclusters deposited on metal oxides are of great practical and fundamental interest in catalysis.[1−10] Gold, a noble metal known for its inertness in bulk, becomes highly active as catalyst for CO oxidation when bound as a nanometer particle to an MgO-defect-rich surface.[10] Small gold clusters soft landed onto a defect-rich-MgO surface are very active toward low temperature oxidation, and it was found that Au_8 was the smallest cluster to show appreciable activity.[4,7] Furthermore, the catalytic activity of small gold clusters (with up to 20 atoms) supported on a surface is extremely size sensitive. Changes in cluster size by even a single atom can dramatically affect the catalytic property of the clusters.[4,7,8] This fact has motivated research[6,11−16] on the molecular mechanisms responsible for this unexpected reactivity.

On the other hand, experimental studies by Landman et al.[4] on surface-supported Au_8 indicate that gold clusters on a defect-rich MgO surface are more active than on a defect-poor surface. Their results also show that the supporting surface plays an important role. In particular, Haruta et al.[5] investigated experimentally the effect of the support on the CO oxidation by Au_n clusters of various sizes, and concluded that the interaction with the support plays an important role. In fact, the nature of contact between the gold particle and the supporting surface was found to be even more important than the particle size. Later studies have indicated that the catalytic properties of supported gold clusters not only depend on the size,[10] but also on the point

* To whom correspondence should be addressed. E-mail: cqs@matrix.super.unam.mx (C.Q.); jureveles@vcu.edu (J.U.R.).
† Facultad de Ciencias, Universidad Nacional Autónoma de México.
‡ Departamento de Supercómputo, DGSCA, Universidad Nacional Autónoma de México.
§ Cinvestav.
|| Virginia Commonwealth University.

10.1021/jp804355z CCC: $40.75
Published on Web 08/27/2008

and extended defects in the substrate where the cluster is stabilized.[4,17,18] The defects trap the metal particle, facilitate the particle growth, enhance the charge transfer from the surface to the adsorbed gold cluster, and promote the metal particle catalytic activity.[4,17]

In order to analyze the structural changes in the adsorbate and substrate, and its effect on their electronic structure as a function of the adsorption site, in this work, we present a study of the structural and electronic properties of Au and Au_2 on an MgO(100) surface employing a DFT cluster embedding approach. Considering that the number of potential trapping site candidates at the MgO surface is large,[19] we have focused on the search of Au and Au_2-substrate equilibrium geometries on four adsorption sites on the MgO(100) surface: on a five coordinated oxygen (O_{5c}) and on a five coordinated Mg (Mg_{5c}) regular terrace sites, on a neutral F_s color center (oxygen vacancy containing two electrons), and on a charged F_s^+ color center (oxygen vacancy containing one electron). Many theoretical studies have been reported on the adsorption of Au and Au_2 over the MgO(100) surface within the density functional theory (DFT) formalism, and incorporating the exchange and correlation effects through various generalized gradient approximations (GGA). These studies have used a variety of methods including a supercell approach with PW91 and RPBE functionals by Molina et al.,[11] supercell with the PW91 functional by Bogigevic et al.,[19] Molina et al.,[20] Del Vitto et al.,[21] Baracaro et al.,[22] and Pachioni et al.,[23] localized atomic orbital supercell and the PBE functional by Conquet et al.,[24] localized atomic orbital cluster embedding approach and the PBEN and BP86 functionals by Neyman et al.[25] and Inntam et al.,[26] respectively, and several isomers have been reported. In this work, we have studied most of the Au and Au_2 isomers reported in the literature under the same conditions (same basis set and numerical procedure) with the intention to compare them; using a DFT cluster embedding approach and localized Gaussian type orbitals. We have examined the Au and Au_2 adsorption energy (E_a), analyzed the formation of the gold dimer from one Au atom already adsorbed on a given site with one gas phase Au atom (E_{dim}), and from one on a given site Au atom and one on O_{5c} adsorbed Au atom (E_b), and analyzed the charge transfer from the surface to the gold atoms at each adsorption site. We did all these studies both at the local density approximation level (LDA), and at the generalized gradient approximation level (GGA). In the next section we describe our theoretical method. In Section III we present the results and discussion, and final conclusions are given in the last section.

II. Theoretical and Computational Methods

A. Cluster Model. The essential features of the cluster-embedding technique used in this study are illustrated in Figure 1. The active cluster that is treated by DFT calculations is the $Au_2Mg_{30}O_{30}$ moiety shown in red and golden. To provide a proper electrostatic environment and boundary conditions, an Evjen array[27] of 1740 point charges surrounds the active cluster so as to form an MgO(100) surface with the Au_2 on top. Details of the development of the method can be found in previous works by Quintanar et al.,[28,29] in which the rumpling and relaxation of the surface were studied through energy cuts, and later trough structure optimizations with equivalent delocalized coordinates in the work of Reveles et al.[30] Here, we have used the later approach, and performed a combination of equivalent and constrained optimizations of selected atoms as described below.

To take into account the rumpling and relaxation of the MgO(100) surface, the structure of the MgO surface was

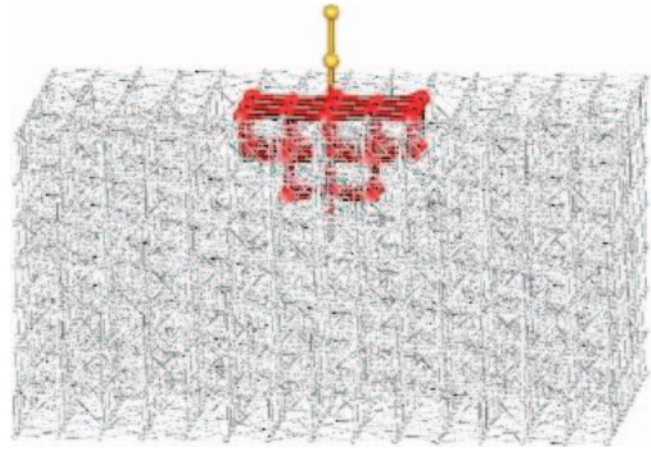

Figure 1. Au_2 particle over an oxygen atom of an embedded $Mg_{30}O_{30}$ cluster. The cluster is centered at an oxygen site of the MgO(100) surface, and the embedding has 1740 point charges.

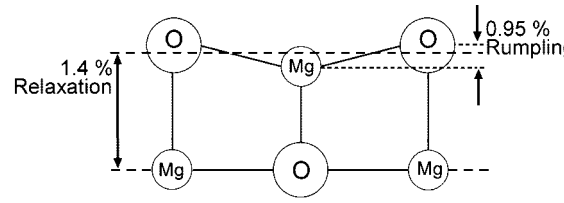

Figure 2. Rumpled and relaxed MgO surface.

initialized from the optimized rumpling and relaxation calculated previously[29,30] as follows: the surface-atom layer of the $Mg_{30}O_{30}$ cluster was rumpled by 0.95% of the interlayer bulk distance, and the rumpled surface layer was then moved along the (100) direction toward the underlying bulk layer by 1.4% of the interlayer bulk distance as depicted in Figure 2.

In order to simulate the adsorption of the Au and Au_2 particles on a regular magnesium or regular oxygen site of the MgO surface, the $Mg_{30}O_{30}$ DFT all electron cluster was initially centered respectively on an Mg or on an O atom. To model the adsorption of Au and Au_2 on the F_s and F_s^+ color centers, a neutral and charged DFT $(Au)Au_2Mg_{30}O_{29}$ cluster centered at the site of an oxygen vacancy was used, respectively. Au and Au_2 were fully optimized without any restrictions, and the surface was studied for two cases. First, the surface was allowed to relax, and second, the surface atoms were fixed. In order to determine the best approach for the case of relaxing the surface we investigated the following possibilities:

a) All the surface atoms were allowed to optimize.

b) The first and second nearest neighbors of the adsorption site were optimized, while the third, fourth and fifth nearest neighbors were kept fixed (Figure 3A).

c) The first and second nearest neighbors of the adsorption site were optimized, while the third, fourth, and fifth nearest neighbors were optimized only along the direction perpendicular to the surface with the equivalent coordinates R_1 (R_2), representing the bond length between an oxygen (magnesium) in the first cluster layer, and a magnesium (oxygen) on the surface (Figure 3A).

In the case (a), we found that during the geometry optimization, the surface atoms of the MgO cluster tend to lose the structure of the solid, and thus, this possibility was discarded. On the other hand, in the cases (b) and (c), the structure of the solid was conserved and yet we were able to study the local relaxation of the first and second nearest neighbor atoms. We chose for the present study the case (c), because it allowed the

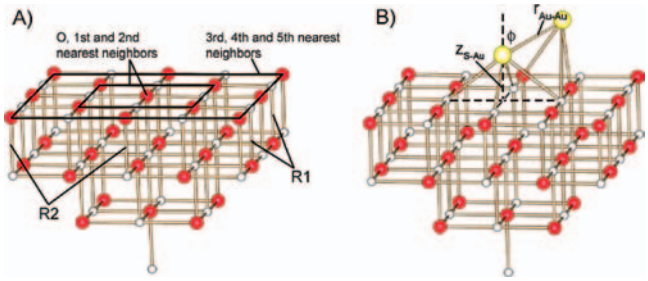

Figure 3. (A) $Mg_{30}O_{30}$ cluster centered at an O site. The first and second nearest neighbors of the Mg at the center are emphasized with a small square, the third, fourth, and fifth with a large square. The two sets (R_1 and R_2) of equivalent coordinates are also shown. Red spheres are oxygen and gray spheres are magnesium atoms. (B) Definition of the geometrical parameters, surface−Au distance (z_{S-Au}), Au−Au distance r_{Au-Au} and the angle from the normal to the surface (tilt angle) ϕ for an $Au_2Mg_{30}O_{29}$ cluster.

maximum relaxation of the surface atoms, and we consider this choice as a good model of the real system.

B. Quantum Chemical Methods. All calculations were performed within the linear combination of Gaussian type orbitals Kohn−Sham (LCGTO-KS) density functional theory code deMon2k.[31] In order to avoid the calculation of four-center electron repulsion integrals, the variational fitting of the Coulomb potential[32,33] was employed. The auxiliary density was expanded in primitive Hermite Gaussian functions employing the A2 function set for Mg and O atoms, and the GEN-A2* function set for Au. All electrons of the MgO cluster were treated explicitly using the DFT optimized double-ζ valence plus polarization (DZVP) basis sets (6321/411/1*) for Mg, and (621/41/1*) for O.[34] For the gold atoms the relativistic effective core potential with 19 valence electrons proposed by Schwerdtfeger et al.,[35] in combination with the correlation consistent aug-cc-pVTZ-pp valence basis set[36] was used. To calculate the exchange-correlation contributions, the LDA approximation as parametrized by Vosko, Wilk, and Nusair,[37,38] and the GGA approximation proposed by Perdew, Burke, and Ernzerhof[39] were employed. The exchange-correlation potential was calculated by a numerical integration on an adaptive grid[40,41] from the auxiliary function density.[42] For the geometry optimization, a quasi-Newton method in internal redundant coordinates with analytical energy gradients was used.[43] The molecular geometries were plotted with the Schakal software.[44] In order to study the charge transfer from the MgO surface to the Au atoms, natural bonding orbital (NBO) atomic charges[45] were calculated at the optimized geometries.

In order to test the reliability of our computational method for gold, several properties of the Au atom as well as the dimer Au_2 were calculated. The ionization potential (IP), and electron affinity (EA) of Au were found in our GGA calculations to be 9.53 and 2.28 eV, respectively, in good agreement with the experimental values of 9.23 and 2.31 eV, respectively.[46] For the gold dimer, we obtained, respectively, an LDA and GGA bond length of 2.45 and 2.51 Å. The experimentally reported gas phase Au_2 bond length is 2.47 Å.[47] Our LDA bond length value is slightly below the experimental value, while our GGA value is slightly above. The LDA and GGA Au_2 binding energy was calculated to be 3.00 and 2.36 eV respectively. While the LDA calculation overestimates the experimental binding energy of 2.30 eV,[48] the GGA calculation is in excellent agreement.

III. Results and Discussion

A. Au_1 and Au_2 Adsorption Energies. In the following sections we present the results of the calculations in which both the Au atoms and the MgO surface were optimized. Later, we discuss the calculations in which the MgO surface atoms were kept fixed, and analyze how these restrictions affected the interaction of the Au particles with the surface.

The adsorption and dimerization energies were calculated in two ways. In one calculation, the geometry was optimized at the GGA level using the PBE functional and the corresponding energies were calculated. The results of these calculations are referred in the Tables as PBE. In the other calculations, we employed a combined approach optimizing the geometry at the LDA level using the VWN functional, and then performing single point energy calculations at GGA level using the PBE functional, from which the corresponding energies were calculated. We refer to this approach as LDA/PBE. The motivation for the combined approach is two-fold. First, some isomers obtained in the LDA optimizations were not minima and optimized to another lower energy isomer in the GGA calculations. Second, our basis set was optimized for LDA functionals, thus, the optimized LDA structures are usually quite reliable, and as a rule of thumb, the experimental bond length lies usually in between the optimized GGA and LDA bond lengths. All our calculated adsorption energies were corrected for the basis set superposition error (BSSE) using the counterpoise method.[49] The uncorrected BSSE values are also given in parenthesis in the tables for comparison.

Following the definition suggested by Del Vitto et al.,[21] the adsorption energy of the gold atom and gold dimer at a specific site was calculated using the equation:

$$E_a = E(Au_n) + E(\text{MgO site}) - E(Au_n\text{MgO site}), \text{ with } (n = 1, 2) \quad (1)$$

where E(Au) is the energy of the gold atom, and $E(Au_n\text{MgO})$, $E(Au_2)$ and E(MgO site) are the energies of the optimized geometries of the respective clusters. Note that according to this convention E_a is positive for a bonded structure, and that a larger E_a implies larger structure stability. The geometrical parameters we use to describe the optimized Au_nMgO clusters are given in Figure 3B.

B. Au Adsorption. ***1. Au on O_{5c} and Mg_{5c}.*** According to our results, the gold atom on the regular MgO terrace prefers to bind on five coordinated oxygen sites O_{5c}. In the case where the Au atom was initially placed on an Mg_{5c} site we found that the Au atom moved toward an adjacent O_{5c} site, and the resulting optimized structure was identical to the one obtained when the Au atom was initially placed on an O_{5c} site. This result is consistent with the reports of Bogigevic et al.,[19] and Del Vitto et al.[21] It is interesting to note that Molina et al.,[11] Barcaro et al.,[22] Pacchioni et al.[23] and Conquet et al.[24] have all reported a stable structure with the Au atom adsorbed on an Mg_{5c} site. However, all these authors agree that the absorption energy of the Au atom on an Mg_{5c} site (0.3 to 0.6 eV) is only half of the E_a of Au on an O_{5c} site.

Optimizing the geometry at PBE level we obtained an E_a of 0.60 eV with an Au-surface distance z_{S-Au} of 2.27 Å. At the LDA/PBE level we obtained a higher E_a of 0.78 eV, and a shorter z_{S-Au} distance of 2.16 Å as expected. These adsorption energies agree fairly well with the reported PBE adsorption energy values of 0.56[11] and 0.78 eV,[24] and are below the reported PW91 adsorption energy of ~0.9 eV.[19,21−23] In general, in all the adsorption sites we found that the PW91 functional predicted larger metal-oxide bond strengths that the ones obtained with other functionals, as previously reported.[20,50]

Our optimized z_{S-Au} distances at PBE level agree reasonably well with most other GGA optimizations reported in the

TABLE 1: BSSE Corrected Adsorption Energies (E_a) and Surface−Au Distances (z_{S-Au}) for the Au Atom Adsorbed on Various Surface Sites at the MgO Surface[a]

		O_{5c} terrace	F_s	F_s^+
E_a (eV)	PBE	0.60 (1.13)	2.53 (3.27)	3.39(4.00)
	LDA/PBE	0.78 (1.57)	2.66 (3.35)	3.41(4.07)
	RPBE[11]	0.56		
	PW91[11]	0.89		
	PW91[19]	0.90	3.12	
	PW91[21]	0.89	3.17	
	PW91[22]	0.87	3.04	3.97
	PW91[23]	1.01		
	PBE[24]	0.78 (1.13)	2.83 (3.25)	
	PBEN[25]		2.88	3.37
z_{S-Au} (Å)	PBE	2.27	1.69	1.50
	LDA/PBE	2.16	1.51	1.37
	PW91[19]	2.34	1.65	
	PW91[21]	2.28	1.79	1.56
	PW91[22]	2.30	1.81	
	PW91[23]	2.24		
	PBE[24]	2.33	1.88	
	PBEN[25]		1.82	1.66

[a] Our PBE and LDA/PBE results calculations underlined. The uncorrected adsorption energies are given in parentheses. Results of previous theoretical studies are also given for comparison.

literature. Nevertheless, fluctuations of more than 5 pm between the different GGA optimizations in this bond length are found. The results collected in Table 1 suggest a z_{S-Au} distance of around 2.30 Å[19,21−24] from the GGA optimizations. Our optimized LDA/PBE value is considerably shorter. Therefore, we believe that 2.30 Å is an upper limit for the z_{S-Au} distance.

2. Au on F_s and F_s^+. In the case of the adsorption of Au on the neutral F_s color center we obtained PBE (LDA/PBE) adsorption energies E_a of 2.53 (2.66) eV, and z_{S-Au} values of 1.69 (1.51) Å. Our adsorption energies showed a fair agreement with the PBE and PBEN values reported respectively by Conquet et al.[24] and Neyman et al.,[25] and were around 20% smaller when compared with the adsorption energy predicted from PW91 calculations[19,21,22] as shown in Table 1. Our optimized z_{S-Au} distance at PBE level is in reasonable agreement with the PW91 calculations of Bogicevic and Jennison.[19] However, the discrepancy to the other GGA calculations is rather large (Table 1). This indicates that the simulation of the adsorption of the Au atom on the color center is not only sensitive to the electronic structure method, but also to the model used to describe the color center in the MgO surface.

It is known that the bonding of metal atoms on metal oxides surfaces becomes much stronger on oxygen vacancies. The results of present calculations shown in Table 1 confirm this finding in that the bonding at the F_s center both with PBE and LDA/PBE is four times stronger than that on the O_{5c} site, and can be rationalized considering that the electrons inside the cavity can be transferred to the adsorbed species. Noting that an Au atom has a high electron affinity, the charge transfer from the surface leads to a strong covalent polar bond. This has recently been confirmed by electron paramagnetic resonance spectroscopy and scanning tunneling microscopy of a single gold atom interacting with the regular and defected MgO (100) surface by Freund et al.[51] Additionally, our analysis of electronic charges is consistent with this picture as discussed below.

For the Au atom adsorption on the charged F_s^+ color center only two previous results exist. Again, our PBE (LDA/PBE) adsorption energies of 3.39 (3.41) eV are in fair agreement with a previous PBEN calculation,[25] whereas our z_{S-Au} distance of 1.50 (1.37 Å) compares favorably well with the previous PW91 calculation[21] (Table 1). As for the F_s color center, no homogeneous picture is obtained from the different theoretical calculations. In the F_s^+ center, the resulting PBE (LDA/PBE) adsorption energies were five times larger than those at the O_{5c} site. This large adsorption energy may be rationalized not only due to the electron charge transfer from the cavity to the adsorbed species, as in the case of the F_s center, but also due to the coupling of the impaired electron at the vacancy with the impaired electron of the Au atom, producing the formation of a strong two center two electron bond.

TABLE 2: Relative Energies (E_{rel}), BSSE Corrected Adsorption Energies (E_a), Dimerization Energies (E_{dim} and E_b), the Surface−Au Distance (z_{S-Au}), Au−Au Distance r_{Au-Au}, and the Tilt Angle (ϕ) for the Adsorption of Au_2 on the O_{5c} Surface Site of the MgO Surface[a]

	E_a (eV)	E_{dim} (eV)	E_b (eV)	z_{S-Au} (Å)	r_{Au-Au} (Å)	ϕ (deg)
PBE	1.05 (1.88)	3.12	1.99	2.14	2.49	5.8
LDA/PBE	1.08 (1.94)	2.71	1.15	2.05	2.44	5.8
RPBE[11]	0.99					
PW91[11]	1.36					
PW91[19]			2.15	2.18	2.53	0.2
PW91[20]	1.48					
PW91[21]	1.49	2.91	1.99	2.18	2.53	6
PW91[22]	1.23			2.31	2.53	
PBE[24]	1.27 (1.61)			2.19	2.56	0.0
BP86[26b]	1.70		1.99	2.14	2.51	

[a] Our PBE and LDA/PBE results are underlined. The uncorrected adsorption energies are given in parentheses. Results of previous theoretical studies are also given for comparison. [b] Includes BSSE correction.

C. Au_2 Dimer Adsorption and Dimerization Energies. The ground-state of the gas phase gold dimer is a singlet, and it has been reported to remain singlet when supported on the MgO surface irrespective of the adsorption site.[21] Following again the definitions of Del Vitto et al.,[21] we calculated the E_{dim} and E_b dimerization energies using the equations:

$$E_{dim} = E(\mathrm{Au}) + E(\mathrm{Au_1/MgO\ site}) - E(\mathrm{Au_2/MgO\ site}), \text{ and}$$

$$E_b = E(\mathrm{Au_1/MgO\ site}) + E(\mathrm{Au_1/MgOO_{5c}}) - E(\mathrm{Au_2/MgO\ site}) - E(\mathrm{MgOO_{5c}})$$

Here E_{dim} is the binding energy of a gas phase Au atom to another Au atom already bound to a given surface site (O_{5c}, Mg_{5c}, F_s or F_s^+), and E_b is the binding energy of a Au atom bound to an O_{5c} site to another Au atom on a given surface site (O_{5c}, Mg_{5c}, F_s or F_s^+). Note that according to this convention, E_{dim} and E_b are positive for a bound structure and larger values of E_{dim} and E_b imply larger structural stability of the Au_2 dimer. In this way, E_b provides a measure of the thermodynamic stability and tendency of two surface absorbed atoms to combine.

D. Au_2 Adsorption. ***1. Au_2 on O_{5c}.*** According to the geometry optimization analysis, we found that Au_2 over O_{5c} possesses only one stable configuration; the dimer almost perpendicular to the surface and slightly tilted from the normal to the surface (tilt angle ϕ) toward the Mg atom by 5.6°. The PBE (LDA/PBE) adsorption energies E_a were calculated to be 1.05 (1.08) eV. These values are in good agreement with the RPBE value reported by Molina et al.[11] of 0.99 eV, and resulted smaller than the PBE value of 1.27 eV reported by Conquet et al.[24] In general, the E_a from PW91 calculations resulted higher (1.23−1.49 eV)[11,20−22] when compared with other functionals, as in the case of the Au adsorption (see Table 2).

However, the largest discrepancy was found with the BP86 results of Intamm et al.[26] who predicted an E_a value of 1.70 eV. The E_{dim} values from PBE (LDA/PBE) calculations show that in binding a gas phase gold atom to an Au atom already adsorbed on an O_{5c} site there is an energy gain of 3.12 (2.71) eV, while the E_b value shows that there is an energy gain of 1.99 (1.15) eV in binding two Au atoms already adsorbed on O_{5c} sites. Our E_{dim} agrees reasonable well with the PW91 value reported by Del Vitto et al.[21] of 2.91 eV, while our E_b is within the range of values 1.99−2.15 eV reported in PW91[19,21] and BP86[26] calculations. Summarizing, the gain in energy in forming a gold dimer over O_{5c} has a large values of 3 eV when an Au atom over an O_{5c} is bound to another Au from the gas phase, and is 2 eV when two Au atoms adsorbed on O_{5c} sites are combined on the surface. Both these values are higher than the adsorption energy of 1 eV for a dimer molecule adsorbed from the gas phase (see Table 2).

For the surface-Au distance z_{S-Au} the PBE (LDA/PBE) calculations gave a value of 2.14 (2.05) Å; for the Au−Au distance r_{Au-Au} a value of 2.49 (2.44) Å, and a ϕ angle of 5.6° (5.6°). The PBE distances are in good agreement with the values reported in PW91,[19,21,22] PBE[24] and BP86[26] calculations (Table 2), while the LDA/PBE distances are consistently smaller. Exceptionally, Barcaro et al.[22] predicted a large z_{S-Au} distance of 2.31 Å. Based on these results, we believe that 2.16 and 2.51 Å are the upper limits for the z_{S-Au} and r_{Au-Au} distances respectively. Our calculated ϕ angle agreed well with the PW91 report of Del Vitto et al.[21] of 6°, however, Bogicevic et al.[19] and Conquet et al.[24] reported smaller tilt angles of 0.2° and 0°, espectively. This discrepancy can be attributed to the sensibility of the optimized geometries with respect to the different models used to describe the adsorption site. Later, we showed that the agreement in the ϕ angle improves in the case of the adsorption of Au_2 over the F_s and F_s^+ color centers, in which cases, the adsorption energies are around two to three times stronger than at the O_{5c} site.

While our finding of only one stable isomer (Au_2 almost perpendicular to the surface) is consistent with references,[11,19,21] and,[23] a few publications have reported another isomer for the Au_2 adsorption on an O_{5c} site. Molina et al.[20] Barcaro et al.,[22] Conquet et al.,[24] and Intamm et al.[26] reported an isomer where the Au_2 molecule is parallel to the surface. Nevertheless, in most of these works[22,24,26] the reported E_a of the parallel isomer was less than half-the E_a of the vertical isomer, while for Molina et al.[20] it was 42% smaller. In our study, when we optimized the Au_2 dimer from an initial position parallel to the surface we found that the dimer tend to move toward the configuration of Au_2 perpendicular to the surface. A parallel isomer was however found when the surface atoms were kept fixed as discussed in the next section.

2. Au_2 on Mg_{5c}. In the case of the adsorption of Au_2 on an Mg_{5c} site we found that when the Au_2 was initially placed perpendicular to the surface, the Au_2 moved away from the Mg_{5c} site toward an adjacent O atom, and the final geometry was almost identical to the one obtained when the Au_2 particle was initially placed on an O_{5c} site. When we optimized the Au_2 dimer from an initial position parallel to the surface over an Mg_{5c} site, we found as in the case of Au_2 over O_{5c} that the dimer tend to move toward the configuration of Au_2 perpendicular to the surface over the O_{5c} site.

On the other hand, in the PBE studies having the surface frozen we found the isomer with Au_2 almost perpendicular to the surface over O_{5c} (vertical isomer), but we also found a stable isomer 0.54 eV higher in energy with the Au_2 parallel to the surface (parallel isomer) on top of an Mg atom, as shown in Figure 4. This relative energy between the vertical and parallel isomers agrees with the value of 0.62 eV reported by Molina et al.[20] The vertical isomer presented an E_a of 0.94 eV, an E_{dim} of 3.09 eV and a E_b of 1.93, while for the parallel isomer the absorption energy was considerably smaller, and E_{dim} and E_b resulted smaller but of comparable magnitude with respect to the vertical isomer, namely E_a of 0.30 eV, E_{dim} of 2.56 and E_b of 1.39 eV. The vertical isomer optimized to a z_{S-Au} of 2.16 Å, r_{Au-Au} of 2.50 Å, and a tilt ϕ angle of 1.6°, while for the parallel isomer the z_{S-Au} distances were of 2.82 and 2.84 Å for the two gold atoms, r_{Au-Au} of 2.56 Å, and the tilt angle ϕ was 91.4°. These results are collected in Table 3 and presented in Figure 4. We can observe in Table 2 for the vertical isomer on an O_{5c} site obtained with the relaxation of the surface, and in Table 3 for the vertical isomer obtained having the surface frozen, that in both cases the energetics and geometrical parameters were almost the same, as both cases correspond to the same final configuration for Au_2.

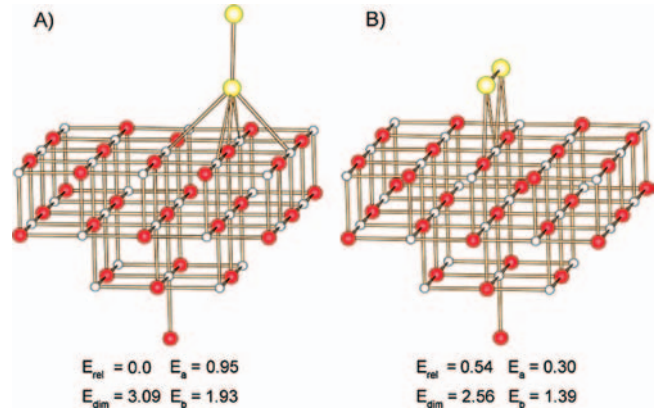

Figure 4. Gold dimer isomers one almost parallel over the Mg_{5c} site of the regular MgO(100) terrace frozen surface (A), and one almost perpendicular that flip over from an Mg_{5c} over an adjacent O_{5c} site (B). E_{rel} is the relative energy with respect to the most stable isomer. E_a, E_{dim} and E_b energies are given in units of eV's.

Comparing our results for the parallel isomer with the reports of Barcaro et al.,[22] Conquet et al.,[24] and Intamm et al.[26] we found that our predicted E_a of 0.30 eV has a good agreement with the BP86[26] reported value of 0.24 eV, but are smaller than the PW91[20,22] and PBE[24] reported values of 0.54, 0.59, and 0.86 eV, respectively.

For the surface-Au distance z_{S-Au} we found large disagreements between the previous studies. Barcaro et al.[22] reported the parallel isomer with the Au_2 dimer on top of a hollow site with z_{S-Au} distances of 2.63 Å for both Au atoms. Conquet et al.[24] reported the parallel isomer without specifying its location (on top of a hollow site, or on top of an Mg atom) with z_{S-Au} distances of 2.52 Å for both Au atoms. Finally, Intamm et al.[26] reported both isomers, Au_2 parallel on top of a hollow site, and on top of an Mg atom as stable configurations. The on top of a hollow site configuration was reported as the most stable one with z_{S-Au} distances of only 2.34 Å for both Au atoms, while the configuration of top of an Mg atom was found to be 0.18 eV higher in energy with z_{S-Au} distances of 2.82 and 2.88 Å. In the present study, we only found the configuration of the parallel isomer on top of an Mg site (Figure 4) with z_{S-Au} distances of 2.82 and 2.84 Å in fair agreement with the high energy isomer reported by Intamm et al. In contrast with the disagreement of the z_{S-Au} distances, for the z_{Au-Au} distance we found a good agreement between our calculated value of 2.56 Å and the PW91[22] and BP86[26] values of 2.56 and 2.59 Å

TABLE 3: Results for the PBE Calculations of Au_2 Over an Mg_{5c} Site Having the MgO Surface Frozen. Relative Energies (E_{rel}), BSSE Corrected Adsorption Energies (E_a), Dimerization Energies (E_{dim} and E_b), Surface−Au Distance (z_{S-Au}), Au−Au Distance r_{Au-Au} and the Tilt Angle (ϕ) for the Adsorption of Au_2 on an Mg_{5c} Site of the MgO Surface[a]

		Au_2 over Mg_{5c} surface frozen	
		vertical	parallel
E_{rel} (eV)	PBE	0.0	0.54
	PW91[20]	0.0	0.62
E_a (eV)	PBE	0.95 (1.90)	0.30 (1.36)
	PW91[20]		0.86
	PW91[22]		0.59
	PBE[24]		0.54 (1.11)
	BP86[26b]		0.24
E_{dim} (eV)	PBE	3.09	2.56
E_b (eV)	PBE	1.93	1.39
z_{S-Au} (Å)	PBE	2.16	2.82 and 2.84
	PW91[22]		2.63 and 2.63
	PBE[24]		2.52 and 2.52
	BP86[26]		2.34 and 2.34
r_{Au-Au} (Å)	PBE	2.50	2.56
	PW91[22]		2.56
	PBE[24]		2.63
	BP86[26]		2.59
ϕ (deg)	PBE	1.6	91.4
	PW91[22]		90
	PBE[24]		90
	BP86[26]		90

[a] Our results are underlined. The uncorrected adsorption energies are given in parentheses. Results of previous theoretical studies are also given for comparison. [b] Includes BSSE correction.

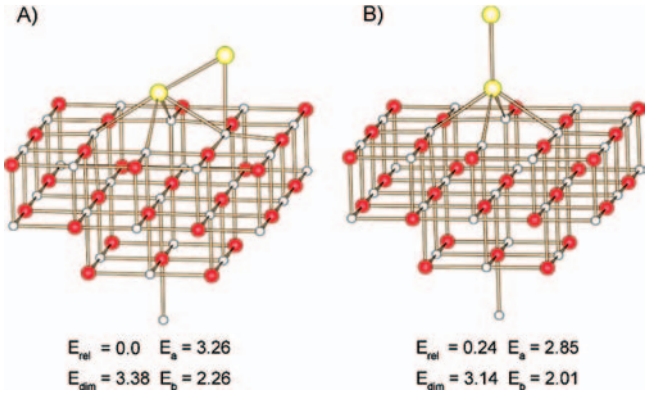

Figure 5. Gold dimer isomers on the F_s color center (A), tilted toward an Mg atom (B), and vertical (C). E_{rel} is the relative energy with respect to the most stable isomer. E_{abs}, E_{dim} and E_b energies are given in units of eV's.

respectively, however, the PBE[24] reported value of 2.63 Å resulted higher. Finally, the tilt angle ϕ agreed in all the previous reported and the present study. In summary, no homogeneous picture is obtained for the z_{S-Au} distances from the different theoretical calculations, while we believe that 2.57 Å can be set as the upper limit for the z_{Au-Au} distance, and 91° for the ϕ angle.

3. Au_2 on F_s (Vacancy with Two Electrons). For the adsorption of the Au_2 over the neutral vacancy F_s we found in our PBE calculations two stable configurations as shown in Figure 5: Au_2 tilted toward a surface Mg atom (Mg-tilted), being the most stable, and the configuration perpendicular to the surface (vertical isomer) 0.24 eV higher in energy. The Mg-tilted isomer had an adsorption energy value E_a of 3.26 eV, an energy gain in the dimerization combining a gas phase gold atom and an on F_s adsorbed gold atom E_{dim} to be 3.38 eV, and

TABLE 4: Relative Energies (E_{rel}), BSSE Corrected Adsorption Energies (E_a), Dimerization Energies (E_{dim} and E_b), Surface−Au Distance (z_{S-Au}), Au−Au Distance r_{Au-Au} and the Tilt Angle (ϕ) for the Adsorption of Au_2 on the F_s Site[a]

		Mg-tilted	O-tilted	vertical
E_{rel} (eV)	PBE	0.0	–	0.24
	LDA/PBE	0.0	0.27	0.32
	PW91[20]	0.0		0.18
	PW91[21]	0.0	0.26	
	PBE[24]	0.0	0.27	0.27
E_a (eV)	PBE	3.26 (4.19)	–	2.85 (4.05)
	LDA/PBE	3.23 (4.28)	2.73 (4.01)	3.02 (3.96)
	PW91[20]	3.76		3.57
	PW91[21]	4.17	3.91	3.89
	PW91[22]			3.72
	PBE[24]	3.49 (4.12)	3.33 (4.00)	3.38 (3.86)
	BP86 [26b]			4.06
E_{dim} (eV)	PBE	3.38	–	3.14
	LDA/PBE	3.27	3.00	2.95
	PW91[21]	3.21		
E_b (eV)	PBE	2.26	–	2.01
	LDA/PBE	1.70	1.43	1.38
	PW91[19]	2.21		
	PW91[21]	2.42		
	BP86[26]			2.11
z_{S-Au} (Å)	PBE	1.20	–	1.49
	LDA/PBE	1.17	1.16	1.35
	PW91[19]	1.53		
	PW91[21]	1.48		
	PW91[22]			1.60
	PBE[24]	1.68	1.66	1.69
	BP86[26]			1.62
r_{Au-Au} (Å)	PBE	2.68	–	2.57
	LDA/PBE	2.61	2.59	2.52
	PW91[19]	2.72		
	PW91[21]	2.73		
	PW91[22]			2.59
	PBE[24]	2.74	2.72	2.62
	BP86[26]			2.63
ϕ (deg)	PBE	58.7	–	0.6
	LDA/PBE	56.3	57.6	0.8
	PW91[19]	56.3		
	PW91[21]	57		
	PBE[24]	59.0	61.0	0.0

[a] Our PBE and LDA/PBE results are underlined. The uncorrected adsorption energies are given in parentheses. Results of previous theoretical studies are also given for comparison. [b] Includes BSSE correction.

an energy gain in the dimerization at expenses of two adsorbed gold atoms (one on an O_{5c} site and another on an F_s site) E_b of 2.26 eV. These results are in good agreement with the PW91[19,21] and PBE[24] reports, although the E_a from the PW91[20,21] reports led to a 25% higher value as shown in Table 4. The vertical isomer had an E_a of 2.85 eV, E_{dim} of 3.14, and an E_b of 2.01 eV. In this case we found a large disagreement between ours and previous reported adsorption energies with values ranging from 2.85 to 4.06 eV showing the strong sensibility of the E_a with respect to the different models employed to describe the adsorption site. In contrast, for the E_b dimerization energy we found a good agreement with the 2.11 eV value reported in BP86 calculations.[26]

From the analysis of the optimized geometries we found for the Mg-tilted isomer a dimer-surface distance z_{S-Au} of 1.20 Å, an Au−Au distance r_{Au-Au} of 2.68 Å, and a ϕ angle of 58.7°. For the z_{S-Au} distance we did not find a homogeneous value, as in this and previous studies the values ranges from 1.20 to 1.68 Å. In the case of the r_{Au-Au} distance and the ϕ angle we

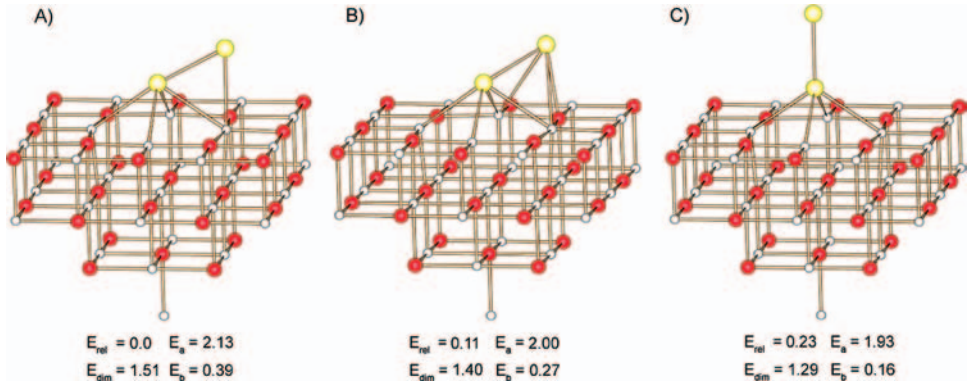

Figure 6. Gold dimer isomers on the F_s^+ paramagnetic color center, tilted toward an Mg atom (A), toward an O atom (B), and vertical (C), E_{rel} is the relative energy with respect to the most stable isomer. E_a, E_{dim} and E_b energies are given in units of eV's.

found a more consistent picture, although fluctuations in r_{Au-Au} of up to 6 pm between the different GGA optimizations were found. Based on these results, we believe that 2.70 Å and 58° can be set as the upper limits for the z_{Au-Au} distance and ϕ angle respectively. For the vertical isomer our PBE calculations predicted a z_{S-Au} distance of 1.49 Å, an r_{Au-Au} of 2.57 Å, and a ϕ angle of 0.6°. As in the case of the Mg-tilted isomer, the z_{S-Au} distance presented large variations between different reports (Table 4), while the r_{Au-Au} and ϕ angle values were more consistent, and allowed us to define upper limits of 2.59 Å and 0.5° for r_{Au-Au} and ϕ respectively.

While our PBE calculations predicted only two stable isomers, the LDA/PBE calculations predicted three stable configurations: the most stable being the Mg-tilted isomer, and 0.27 and 0.32 eV higher in energy the isomers with the dimer tilted toward a surface oxygen (O-tilted), and the vertical isomer respectively. In general, the adsorption and dimerization LDA/PBE energies were smaller when compared with the PBE results with the largest difference found for E_b as shown in Table 4. This finding of underestimation of the adsorption and dimerization energies, and particularly of E_b by the LDA/PBE calculations was also observed for the adsorption of Au_2 on an O_{5c}, on an F_s site and on an F_s^+ site as discussed later.

The finding of only two stable configurations (Mg-tilted and vertical isomer) in our PBE calculations is consistent with the reports of Bogicevic et al.,[19] Molina et al.,[20] Barcaro et al.[22] and Inntam et al.;[26] while Del Vitto et al.[21] and Conquet et al.[24] additionally reported the O-tilted configuration. According to Molina et al. the Mg-tilted isomer is the most stable configuration and the vertical isomer lies 0.18 eV higher in energy, Del Vitto et al. reported the Mg-tilted isomer being the most stable configuration and the O-tilted isomer 0.26 eV higher in energy, and finally, also Conquet et al. find the Mg-tilted to be the most stable isomer and the O-tilted and vertical isomers to be 0.27 eV higher in energy. Thus, our relative energies show an excellent agreement with these reports.

According with the LDA/PBE calculations the O-tilted isomer had an E_a of 2.73 eV, an E_{dim} of 3.0 eV, and an E_b of 1.43 eV. Our calculated E_a and the previous reported adsorption energies reported large variations with values ranging from 2.73 to 3.33 eV (Table 4). From the analysis of the optimized geometries, for the Mg-tilted and vertical isomers we found similar but smaller geometrical parameters in the LDA/PBE results (as they correspond to VWN optimizations) when compared with the PBE calculations. For the O-tilted isomer the LDA/PBE calculation predicted a z_{S-Au} distance of 1.16 Å, a r_{Au-Au} of 2.59 Å and a ϕ angle of 57.6°. The distances resulted much smaller than the PBE reported values of Conquet et al.[24] and thus we were not able to establish any limit for them.

In summary, all the isomers in both PBE and LDA/PBE calculations presented large E_a, E_{dim} and E_b energies, indicating that the metal particle is strongly bonded to the surface, and may not diffuse when it is adsorbed on a neutral F_s color center, but it can easily grow to dimer from one on F_s absorbed Au atom, and either from one gas phase or one on O_{5c} adsorbed gold atom. Considering the small relative energy differences between the isomers predicted by our calculations, we think that their probability to be present in the real system should be almost the same; they may coexist at very low temperature, while at finite temperature they will rapidly interchange.

4. Au_2 on F_s^+ (Vacancy with One Electron). We found that both PBE and LDA/PBE calculations predicted for the F_s^+ adsorption site three stable configurations as shown in Figure 6. According to the PBE calculations, the Mg-tilted isomer was found to be the most stable configuration and 0.11 and 0.23 eV higher in energy were found, respectively the O-tilted and vertical isomers. In the LDA/PBE calculations the O-tilted isomer was found to be the most stable isomer and 0.15 and 0.23 eV higher in energy, were found the Mg-tilted and vertical isomers respectively (Table 5). Given the small relative energy differences, we expect the three isomers to coexist in a rapid interchange in the real system at finite temperatures.

The PBE calculations predicted, for the Mg-tilted isomer, an E_a of 2.13 eV, an E_{dim} of 1.51 eV and an E_b of 0.39 eV. For the O-tilted isomer, they predicted an E_a of 2.00 eV, an E_{dim} of 1.40 eV, and an E_b of 0.27 eV, and finally, for the vertical isomer an E_a of 1.93 eV, an E_{dim} of 1.29 eV, and an E_b of 0.16 eV. In previous studies, Del Vitto et al.[21] reported only the Mg-tilted isomer, while Inntam et al. reported only the vertical isomer.[26] In the case of the Mg-tilted isomer, our calculated E_a presented a large difference when compared with the PW91[21] reported value, while E_{dim} and E_b showed a fair agreement as shown in Table 5.

For the vertical isomer our calculated E_a presented a large difference when compared with the BP86[26] reported E_a value. In the case of our calculated E_b we obtained a value of 0.16 eV considerably smaller when compared with the other adsorption sites (1.4−2.2 eV), while Inntam et al.[26] reported a negative E_b of −0.04 eV. For the LDA/PBE calculations although E_a and E_{dim} were smaller but very close to the PBE values, E_b was predicted to be negative in the range of −0.16 to −0.41 eV for the three isomers, thus implying the dissociation of the Au_2 dimer. Interestingly, a similar result was found in the calculations where the surface was kept fixed, as discussed below.

From the analysis of the optimized geometries, the PBE (LDA/PBE) calculations predicted for the Mg-tilted isomer an z_{S-Au} of 1.49 (1.44) Å, an r_{Au-Au} of 2.64 (2.58) Å, and a ϕ angle of 61.2° (62.2°). For the O-tilted isomer with a similar

TABLE 5: Relative Energies (E_{rel}), BSSE Corrected Adsorption Energies (E_a), Dimerization Energies (E_{dim} and E_b), Surface−Au Distance (z_{S-Au}), Au−Au Distance r_{Au-Au} and the Tilt Angle (ϕ) for the Adsorption of Au_2 on the F_s^+ Site[a]

F_s^+ site		Mg-tiled	O-tilted	vertical
E_{rel} (eV)	PBE	0.0	0.11	0.23
	LDA/PBE	0.15	0.0	0.11
E_a (eV)	PBE	2.13(3.15)	2.00(3.04)	1.93(2.92)
	LDA/PBE	1.97(3.15)	1.80(3.00)	1.89(2.89)
	PW91[21]	2.82		
	BP86[26b]			2.40
E_{dim} (eV)	PBE	1.51	1.40	1.29
	LDA/PBE	1.41	1.26	1.15
	PW91[21]	1.17		
E_b (eV)	PBE	0.39	0.27	0.16
	LDA/PBE	−0.16	−0.30	−0.41
	PW91[21]	0.26		
	BP86[26]			−0.04
z_{S-Au} (Å)	PBE	1.49	1.48	1.52
	LDA/PBE	1.44	1.36	1.35
	PW91[21]	1.42		
	BP86[26]			1.62
r_{Au-Au} (Å)	PBE	2.64	2.69	2.59
	LDA/PBE	2.58	2.67	2.52
	PW91[21]	2.64		
	BP86[26]			2.60
ϕ (deg)	PBE	61.2	69.4	1.1
	LDA/PBE	62.2	72.7	1.2
	PW91[21]	60		

[a] Our PBE and LDA/PBE results are underlined. The uncorrected adsorption energies are given in parentheses. Results of previous theoretical studies are also given for comparison. [b] Includes BSSE correction.

geometry, the calculations predict an z_{S-Au} of 1.48 (1.36) Å, an r_{Au-Au} of 2.69 (2.67) Å, and a ϕ angle of 69.4° (72.7°), and finally, for the vertical isomer an z_{S-Au} of 1.52 (1.35) Å, an r_{Au-Au} of 2.59 (2.52) Å, and a ϕ angle of 1.1° (1.2°). For the Mg-tilted isomer the z_{S-Au} qualitatively agreed with PW91[21] with a difference of 7 pm, while the r_{Au-Au} and ϕ angle presented a good agreement both in the Mg-tilted and vertical isomers with the PW91[21] and BP86[26] reports. Based on theses results we define the upper limits of 2.62 Å and 0.5° for r_{Au-Au} and ϕ respectively in the Mg-tilted isomer, and 2.60 Å for r_{Au-Au} in the vertical isomer.

In summary, for all the isomers (Mg-tilted, O-tilted and vertical) we found large E_a and E_{dim}, but a very small E_b indicating that the metal particle is strongly bonded to F_s^+ center, can grow at expenses of one Au atom adsorbed on the F_s^+ center or one Au gas phase atom, but once formed, the dimer can easily break giving a gold atom to an O_{5c} site, given that binding energy of the dimer (E_b) is very small, and even negative in the case of the LDA/PBE calculations.

E. Calculation of Au_2 on a Frozen MgO Surface. Our calculations where the surface was kept frozen and the gold dimer was fully free produced similar results as those obtained with the ones where the surface was allowed to relax, with the exception of the cases of Au_2 over Mg_{5c} and F_s^+ sites. PBE calculations having the surface frozen predicted for the optimized geometry of Au_2 over F_s^+ an Au−Au distance of 3.45 Å, leading to the breaking of the dimer, leaving one gold atom over the F_s^+ center and the other adsorbed on one Mg_{5c} site tilted toward an oxygen atom. Remembering that our results for the F_s^+ center where the surface was allowed to relax predicted a very small E_b for PBE, and a negative E_b for LDA/PBE calculations, implying that at this site the dimer can easily dissociate, we think that the structural restrictions introduced by freezing the surface are indeed able to produce the dissociation of the dimer. Consequently, although we obtain different results when the surface is allowed to relax or when the surface was kept frozen, they are consistent with each other; one predicts a high probability for dimer breaking, while the other predicts the breaking of the dimer.

TABLE 6: Calculated NBO Atomic Charges at the Au Atoms for the Different Adsorption Sites[a]

		q (Au)	
Au on O_{5c}	PBE	−0.13	
Au on F_s^+	PBE	−0.60	
	PBE[24]	−0.31	
	BP86[25]	−0.42	
Au on F_s	PBE	−0.82	
	PBE[24]	−1.12	
	BP86[25]	−0.85	
		q (Au_I)	q (Au_{II})
Au_2 on O_{5c}			
vertical	PBE	−0.01	−0.17
Au_2 on Mg_{5c}			
vertical	PBE	−0.03	−0.14
parallel	PBE	0.07	−0.04
Au_2 on F_s^+			
Mg tilted	PBE	−0.50	−0.10
O tilted	PBE	−0.54	−0.09
vertical	PBE	−0.63	−0.02
Au_2 on F_s			
Mg tilted	PBE	−0.59	−0.61
vertical	PBE	−0.66	−0.55

[a] For the Au_2 dimer, Au_I is the gold atom nearest to the surface, while Au_{II} is the farthest one. Our PBE results are underlined. Results of previous theoretical studies are also given for comparison.

F. Charge Transfer at the Different Adsorption Sites. As mentioned in the introduction, it has been shown that the catalytic properties of gold clusters critically depend on the charge of the clusters at the metal-oxide interface.[10] Sanchez et al.[4] and Hakkinen et al.[10] have reported that for Au_8, the first cluster size that shows appreciable catalytic activity toward low-temperature oxidation of CO on a defect rich MgO surface that charging by a surface F_s color center is crucial for the O_2 binding, and thus, for its catalytic activity. When comparing defect sites, an enhancement of charge transfer is expected at the F_s site as it contains two trapped electrons, compared with the F_s^+ site with only one trapped electron, and O_{5c} with not trapped electrons. Experimental studies from Freund et al.[51] based on the analysis of the infrared (IR) stretching of CO molecules attached to Au particles adsorbed on color centers, and regular terrace sites have been interpreted that the Au particles on color centers are charged, while Au particle on regular terrace sites are neutral. Molina et al.,[11] and Del Vitto et al.[21] have employed charge density plots to analyze the charge transfer at different adsorption sites, while Conquet et al.[24] and Neyman et al.[25] have calculated Bader[52] and potential derived charges respectively. In this study we have calculated NBO atomic charges[45] for the optimized geometries at the different adsorption sites. Table 6 presents the calculated charges and also gives the charges given in references[24] and[25] for comparison. We can observe that we correctly predict the charge transfer trend with charges of −0.13, −0.6 and −0.8 for the adsorption of Au at the O_{5c}, F_s, and F_s^+ sites respectively. Although calculated with different methods, the charges previously reported qualitatively agree with our results. In the case of the Au_2 dimer, the sum of the charge on both Au atoms again

produce the expected trend with −0.2, −0.6 and −1.1 electronic charges respectively at the O_{5c}, F_s^+ and F_s sites.

IV. Conclusions

To summarize, we have analyzed several isomers of Au and Au_2 over different adsorption sites of MgO(100) that have been reported in the literature with a variety of theoretical methods. Using the same theoretical method and a DFT cluster embedding approach, we were able to compare our results with the previous reports and to establish in most of the cases limits for the adsorption, binding energies, and geometrical parameters.

Additionally, our analysis allowed us to establish the relative energy ordering of the isomers from the most stable to the least stable one as well as the charge transfer from the MgO surface to the Au atoms at each adsorption site. We further find that for a given site, many isomers are almost degenerate and that the probability of finding them in the experimental system is almost the same, indicating that they may even coexist at very low temperatures, while a rapid interchange is expected at finite temperatures.

The calculations where the surface was kept frozen and the gold dimer was fully free led to similar results as those obtained with the ones where the surface was allowed to relax, with the exception of the cases of Au_2 over and Mg_{5c} and F_s^+ sites. In general, both fully generalized gradient and combined calculations produced similar results with the exception of the F_s and F_s^+ adsorption sites.

For the adsorption on the O_{5c} site our studies found one stable configuration with the Au_2 almost perpendicular to the surface, and show that this site promotes the particle growth. Our studies of Au_2 over an Mg_{5c} site with a frozen MgO surface predict two isomers, one with the dimer perpendicular with a configuration similar to the case of Au_2 adsorbed on an O_{5c} site, and one 0.54 eV higher in energy with the dimer parallel to the surface.

For the vacancy with two electrons F_s site, two configurations were found as local minima, Au_2 tilted toward a surface Mg being the most stable, and 0.24 eV higher in energy an isomer with the Au_2 perpendicular to the surface. The Mg tilted isomer presented the largest adsorption and dimerization energies, and according to our results, on this site an Au atom is strongly adsorbed and is likely to grow to form a dimer. In this site, the LDA/PBE combined calculations predicted the existence of another low lying energetic isomer with the Au_2 dimer tilted toward an O atom.

For the vacancy with one electron, we found three configurations that represent local minima, Au_2 tilted toward Mg being the most stable and tilted toward O and perpendicular to the surface respectively 0.11 and 0.23 eV higher in energy. On the F_s^+ site we find that the Au_2 dimer may not be stable as it presented small binding energy. In this site, the LDA/PBE calculations predicted that the isomer with a tilted O atom was the most stable configuration, and that 0.15 and 0.26 higher in energy respectively are the Mg tilted and vertical isomers. The LDA/PBE calculations also predicted the dissociation of the adsorbed Au_2 dimer.

Finally, our charge transfer analysis based of NBO charges showed an increase in the charge transfer from the MgO surface to the Au atoms according to the number of localized electrons at the adsorption sites. Studies on larger Au clusters are currently being performed in order to study the electronic and structural properties of these systems.

Acknowledgment. R.C. and C.Q. acknowledge financial support by the PAPIIT-UNAM IN118806 project and PUNTA-UNAM project. A. M. K. gratefully acknowledges support from the CONAC$_y$T project 60117-U. S.N.K. acknowledges financial support from the Department of Energy (DE-FG02-02ER46009) and JUR acknowledges support from Air Force Office of Scientific Research grant FA9550-05-1-0186. Part of the calculations were performed on the computational equipment of DGSCA UNAM, particularly at the super computer KanBalam.

References and Notes

(1) Haruta, M.; Tsubota, S.; Kobayashi, T.; Kageyama, H.; Genet, M. J.; Delmon, D. *J. Catal.* **1993**, *144* (1), 175–192.
(2) Giordano, L.; Carrasco, J.; Di Valentin, C.; Illas, F.; Pacchioni, G. *J. Chem. Phys.* **2006**, *124* (17), 174709.
(3) Haruta, M. *Nature* **2005**, *437* (7062), 1098–1099.
(4) Sanchez, A.; Abbet, S.; Heiz, U.; Schneider, W.-D.; Häkkinen, H.; Barnet, R. N.; Landman, U. *J. Phys. Chem. A* **1999**, *103* (48), 9573–9578.
(5) Okumura, M.; Tsubota, S.; Haruta, M. *J. Mol. Cat. A: Chem.* **2003**, *199* (1−2), 73–84.
(6) Kim, Y. D.; Fischer, M.; Ganteför, G. *Chem. Phys. Lett.* **2003**, *377* (1−2), 170–176.
(7) Heiz, U.; Sanchez, A.; Abbet, S.; Schneider, W.-D. *Chem. Phys.* **2000**, *262* (1), 189–200.
(8) Walter, M.; Häkkinen, H. *Phys. Rev. B* **2005**, *72* (20), 205440.
(9) Freund, H.-J. *Surf. Sci.* **2002**, *500* (1−3), 271–299.
(10) Yoon, B.; Häkkinen, H.; Landman, U.; Wörz, A.; Antonietti, J.-M.; Abbet, S.; Judai, K.; Heiz, U. *Science* **2005**, *307* (5708), 403–407.
(11) Molina, L. M.; Hammer, B. *Phys. Rev. B* **2004**, *69* (15), 155424.
(12) Valden, M.; Lai, X.; Goodman, D. W. *Science* **1998**, *281* (5383), 1647–1650.
(13) Walter, M.; Häkkinen, H. *Phys. Rev. B* **2005**, *72* (20), 205440.
(14) Markovits, A.; Paniagua, J. C.; López, N.; Minot, C.; Illas, F. *Phys. Rev. B* **2003**, *67* (11), 115417.
(15) Di Valentin, C.; Giordano, L.; Pacchioni, G.; Rosch, N. *Surf. Sci.* **2005**, *522* (1−3), 175–184.
(16) Carrasco, J.; Lopez, N.; Illas, F.; Freund, H.-J. *J. Chem. Phys.* **2006**, *125* (7), 074711.
(17) Sanchez, A.; Abbet, S.; Heiz, U.; Schneider, W.-D.; Ferrari, A. M.; Pacchioni, G.; Rösch, N. *J. Am. Chem. Soc.* **2000**, *122* (14), 3453–3457.
(18) Bäumer, B.; Freund, H.-J. *Prog. Surf. Sci.* **1999**, *61* (7−8), 127–198.
(19) Bogicevic, A.; Jennison, D. R. *Surf. Sci.* **2002**, *515* (2−3), L481–L486.
(20) Molina, L. M.; Alonso, J. A. *J. Phys. Chem. C* **2007**, *111* (18), 6668–6677.
(21) Del Vitto, A.; Pacchioni, G.; Delbecq, F. O.; Sautet, P. *J. Phys. Chem. B* **2005**, *109* (16), 8040–8048.
(22) Barcaro, G.; Fortunelli, A. *J. Chem. Theory Comput.* **2005**, *1* (5), 972–985.
(23) Pacchioni, G.; Giordano, L.; Baistrocchi, M. *Phys. Rev. Lett.* **2005**, *94* (22), 226104.
(24) Conquet, R.; Hutchings, G. J.; Taylor, S. H.; Willock, D. J. *J. Mater. Chem.* **2006**, *16* (20), 1978–1988.
(25) Neyman, K. M.; Inntam, C.; Matveev, A. V. et al. *J. Am. Chem. Soc.* **2005**, *127* (33), 11652–11660.
(26) Inntam, C.; Moskaleva, L. V.; Neyman, K. M.; Rosch, N. *Appl. Phys. A: Mater. Sci. Process.* **2006**, *82* (1), 181–189.
(27) Evjen, H. M. *Phys. Rev.* **1932**, *39*, 675–687.
(28) Quintanar, C.; Caballero, R.; Köster, A. M. *Int. J. Quantum Chem.* **2004**, *96* (5), 483–491.
(29) Quintanar, C.; Caballero, R.; Castaño, V. M. *Int. J. Quantum Chem.* **2005**, *102* (5), 820–828.
(30) Reveles, J. U.; Khanna, S. N.; Köster, A. M. *J. Mol. Struct. (THEOCHEM)* **2006**, *762* (1−3), 171–178.
(31) Köster, A. M.; Calaminici, P.; Casida, M. E.; Flores-Moreno, R.; Geudtner, G.; Goursot, A.; Heine, T.; Ipatov, A.; Janetzko, F.; M. del Campo, J.; Patchkovskii, S.; Reveles, J. U.; Salahub, D. R.; Vela, A. *deMon2k*, V. 2.3.6; The deMon Developers Community: Cinvestav, México, 2006. Available at: www.deMon-software.com.
(32) Dunlap, B. I.; Connolly, J.; W, D.; Sabin, J. R. *J. Chem. Phys.* **1979**, *71* (12), 4993–4999.
(33) Mintmire, J. W.; Dunlap, B. I. *Phys. Rev. A* **1982**, *25* (1), 88–95.
(34) Godbout, N.; Salahub, D. R.; Andzelm, J.; Wimmer, E. *Can. J. Chem.* **1992**, *70* (2), 560–571.
(35) Schwerdtfeger, P.; Dolg, M.; Schwarz, W. H. E.; Bowmaker, G. A.; Boyd, P. D. W. *J. Chem. Phys.* **1989**, *91* (3), 1762–1774.
(36) http://www.emsl.pnl.gov/forms/basisform.html.
(37) Vosko, S. H.; Wilk, L.; Nusair, M. *Can. J. Phys* **1980**, *58* (8), 1200–1211.
(38) Wilk, L.; Vosko, S. H. *J. Phys. C: Solid State Phys* **1982**, *15* (10), 2139–2150.

(39) Perdew, J. P.; Burke, K.; Ernzerhof, M. *Phys. Rev. Lett.* **1996**, *77* (18), 3865–3868.
(40) Krack, M.; Köster, A. M. *J. Chem. Phys.* **1996**, *108* (8), 3226–3234.
(41) Köster, A. M.; Flores-Moreno, R.; Reveles, J. U. *J. Chem. Phys.* **2004**, *121* (2), 681–690.
(42) Köster, A. M.; Reveles, J. U.; M. del Campo, J. *J. Chem. Phys.* **2004**, *121* (8), 3417–3424.
(43) Reveles, J. U.; Köster, A. M. *J. Comput. Chem.* **2004**, *25* (2), 1109–1116.
(44) Keller, E. *Chemie in unserer Zeit* **1980**, *14(2)*, 56−60. http://www.krist.uni-freiburg.de/ki/Mitarbeiter/Keller/schakal.html.
(45) Glendening, E. D.; Badenhoop, J. K.; Reed, A. E.; Carpenter, J. E.; Bohmann, J. A.; Morales, C. M.; Weinhold, F. *NBO 5.G*, Theoretical Chemistry Institute, University of Wisconsin, Madison, WI, 2004; http://www.chem.wisc.edu/∼nbo5.
(46) Huber, H.; Herzberg, G. *Molecular Spectra and Molecular Structure IV Constants Diatomic Molecules*; Van Nostrand: New York, 1979.
(47) Wesendrup, R.; Laerdahl, P.; Swerdtfeger, P. *J. Chem. Phys.* **1999**, *110* (9), 9457–9462.
(48) Morse, M. D. *Chem. Rev.* **1986**, *86* (6), 1049–1109.
(49) Boys, S. F.; Bernardi, F. *Mol. Phys.* **1970**, *19* (4), 553–&.
(50) Giordano, L.; Baistrocchi, M.; Pacchioni, G. *Phys. Rev.* **2005**, *72*, 115403.
(51) Sterrer, M.; Yulikov, M.; Fischbach, E.; Heyde, M.; Rust, H. P.; Pacchioni, G.; Risse, T.; Freund, H. J. *Angew. Chem., Int. Ed.* **2006**, *45*, 2630–2632.
(52) Bader, R. *Atoms in Molecules: A Quantum Theory*; Oxford University Press: New York, 1990.

JP804355Z